Shape from Shading and Intensity Gradient

José R.A. Torreão

Instituto de Computação, Universidade Federal Fluminense
24210-240 Niterói, RJ, Brazil
jrat@ic.uff.br

Abstract. We present a new algorithm for shape estimation, using both brightness and brightness gradient as input data. Our algorithm is an improvement of the recently introduced Green's function approach to shape-from-shading (GSFS). In GSFS, we assume that the single brightness image will be matched to a second image through a uniform disparity field, and solve for the matching image via Green's function. When a linear expansion of the reflectance map is considered, the matching image can be related to surface gradient, leading to a closed-form depth map whose free parameters are easily estimated. Here we show that the same procedure can be repeated with the gradient image as input; a second depth estimate thus results which takes into account higher-frequency components of the imaged surface. Extensive experimentation with synthetic and real images corroborates the advantage of the new method.

1 Introduction

Shape-from-shading (SFS) is a computer vision technique which takes a single shading image as input. In SFS, the goal is to estimate surface orientation, or surface depth, through the image irradiance equation, which relates image intensity to surface gradient via the reflectance map function. Several approaches have been proposed for SFS, most of them relying on simplifying assumptions, such as a lambertian imaging model and known point source illumination; a good survey of the state of the art, as of 1999, can be found in [1].

Recently, we have introduced a novel SFS algorithm, one which is less dependent on restraining conditions: the so-called Green's function shape-from-shading (GSFS) [2]. GSFS has been inspired by the disparity-based approach to photometric stereo (DBPS) [3], a process whereby a pair of photometric stereo images (monocular images acquired under different illuminations) is matched to yield a disparity field similar to those obtaining in stereoscopy [4], from which a depth map for the imaged surface can be recovered. The disparities in DBPS arise from the displacement of the irradiance pattern over the scene, due to the change in illumination direction. As shown in [5], it is possible, under quite general conditions, to adequately model such displacement as a non-uniform rotation, whose parameters can be found via a structure-from-motion estimation. DBPS therefore allows surface reconstruction even in the absence of reflectance-map information.

Similarly to DBPS, the Green's function SFS is based on an irradiance conservation equation, which we introduce assuming that the input image will be matched to a second image through a uniform disparity field. Such equation can be solved via Green's function, yielding a matching image in terms of which a closed-form approximate expression for the surface function can be obtained. The same structure-from-motion approach of [5] can then be applied for the estimation of reflectance map parameters.

The Green's function SFS thus allows shape recovery from input images acquired under loosely controlled conditions, and for unkown reflectance maps. The algorithm has, nevertheless, a tendency to miss finer details of the imaged surface, what is probably due to the fact that it relies on a first-order expansion of the reflectance map, and that second derivatives of the surface function are neglected.

In order to improve the performance of GSFS, we here propose to bring into play the gradient of the brightness function. The use of the intensity gradient for shape estimation has recently been advocated by Zhang and Shah, which incorporated the directional derivatives as a constraint in an optimization strategy, abandoning the traditional brightness factor [6]. In contrast, we here consider shading and gradient cojointly, by showing that the GSFS procedure can be repeated with the gradient data as input, to yield a second surface function estimate. Since this new estimate is based on a second-order expansion of the reflectance map, and takes into account the second derivatives of the depth function, its incorporation leads to a more faithful representation of the higher-frequency components of the scene, as proved by our experiments.

0-7695-0878-2/00 $10.00 © 2000 IEEE

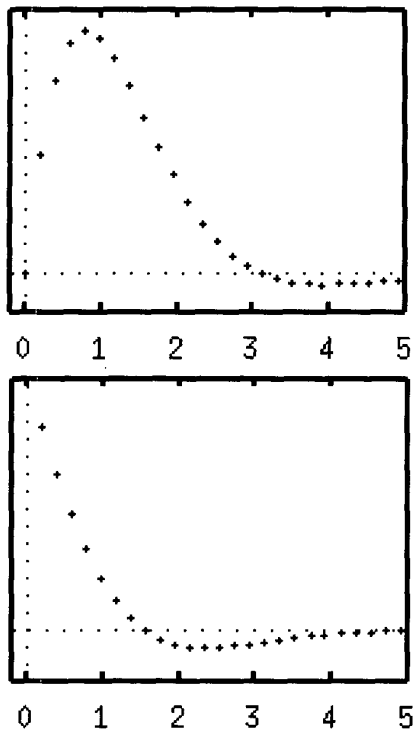

Fig. 1: Top: Filter $G(\xi) \times \xi/u$, Bottom: Filter $\overline{G}(\xi) \times \xi/u$ (Not normalized. Arbitrary vertical scales)

In the following section, we briefly present the Green's function approach to SFS. Following that, we show how to incorporate brightness gradient information into the reconstruction. Next, we present and discuss the experimental results, and conclude with our final remarks.

2 The Green's Function SFS

The rationale of the Green's function SFS can be easily grasped, but its actual derivation is somewhat involved. In what follows, we restrict ourselves to the main points in the development, referring the reader to [2] for the missing details.

We deal with a uniform-albedo surface whose image I_1 is available, and seek a second image, I_2, to match the first, such that $I_1(X,Y) = I_2(X+u, Y+v)$ up to second order in the small disparity components, u and v. Assuming these to be uniform and writing $v = \gamma u$, for $u \neq 0$, we get the following equation for I_2,

$$\frac{\partial^2 I_2}{\partial X^2} + \gamma^2 \frac{\partial^2 I_2}{\partial Y^2} + 2\gamma \frac{\partial^2 I_2}{\partial X \partial Y} + \\ + \frac{2}{u}\left(\frac{\partial I_2}{\partial X} + \gamma \frac{\partial I_2}{\partial Y}\right) + \frac{2}{u^2} I_2 = \frac{2}{u^2} I_1, \qquad (1)$$

which the change of variables

$$X = x, \quad Y = y + \gamma x \qquad (2)$$

reduces to

$$\frac{\partial^2 I_2}{\partial x^2} + \frac{2}{u}\frac{\partial I_2}{\partial x} + \frac{2}{u^2} I_2 = \frac{2}{u^2} I_1 \ . \qquad (3)$$

A solution for $I_2(x, y+\gamma x)$, assuming y fixed, can be found from (3) in the form

$$I_2(x, y+\gamma x) = \int_{\mathcal{D}} G(x-x') I_1(x', y+\gamma x') dx', \quad (4)$$

where $\mathcal{D}$, which can be a function of y, is the domain of interest along x. In (4), $G(x-x')$, called the Green's function, is the solution to the equation

$$\frac{\partial^2 G}{\partial x^2} + \frac{2}{u}\frac{\partial G}{\partial x} + \frac{2}{u^2} G = \frac{2}{u^2}\delta(x-x'), \qquad (5)$$

where $\delta(\cdot)$ is Dirac's delta function [7].

Taking $\mathcal{D}$ as the whole real axis (see [2] for remarks on finite image domains), bounded solutions to (5), for $u > 0$, can be found as (Fig. 1)

$$G(x-x') = \begin{cases} \frac{2}{u}\sin\left(\frac{x-x'}{u}\right)\exp\left\{-\left(\frac{x-x'}{u}\right)\right\} & x > x' \\ 0 & x < x' \end{cases} \qquad (6)$$

Now, let us assume that the irradiance function $I_1(X,Y)$ can be adequately expressed, in terms of surface gradient, through a linear expansion of the reflectance-map function, of the form

$$I_1(X,Y) = k_0(Y-\gamma X) + k_1(Y-\gamma X)P + k_2(Y-\gamma X)Q, \qquad (7)$$

where

$$P \equiv \frac{\partial Z}{\partial X} \ \text{ and } \ Q \equiv \frac{\partial Z}{\partial Y} \qquad (8)$$

are the gradient components of the imaged surface, $Z(X,Y)$. In (7), the parameters k_0, k_1 and k_2 are constant along the lines $Y = \gamma X + \beta$, for constant β, a dependence that can be obtained by taking the reflectance map expansion about local orientations (P_0, Q_0) fixed along those lines.

Now, it is easy to show that a coordinate transformation such as (2) reduces equation (7) to the form

$$I_1(x, y+\gamma x) = k_0(y) + k_1(y) p(x, y+\gamma x), \qquad (9)$$

as long as $\gamma \equiv v/u = k_2(y)/k_1(y)$, where $p = \partial Z/\partial x$. We can thus take equation (9) into equation (4), to obtain

$$I_2(x, y+\gamma x) = k_0(y) \int_0^\infty G(\xi) d\xi +$$

$$+k_1(y)\int_0^\infty G(\xi)p(x-\xi,y+\gamma(x-\xi))d\xi, \qquad (10)$$

where the change of variables $\xi = x - x'$ has been performed.

Since G is normalized to 1 in $[-\infty,\infty]$, it follows from (9) and (10) that

$$k_1(y)p(x,y+\gamma x) = \Delta I(x,y+\gamma x)+$$
$$+k_1(y)\int_0^\infty G(\xi)p(x-\xi,y+\gamma(x-\xi))d\xi, \qquad (11)$$

where $\Delta I = I_1 - I_2$. Given I_1, and with I_2 obtained through (4), equation (11) represents an integral equation for p at each domain point. In order to avoid the need to explicitly solve such equation, we attempt to rewrite the integral factor there in terms of the difference image, ΔI. We start by substituting for p, in the integrand, from equation (11) itself, now at the coordinate $(x-\xi)$. After some tedious manipulation, which at one point involves neglecting the derivative of p with respect to x, we finally arrive at the approximation

$$k_1(y)p(x,y+\gamma x) = \Delta I(x,y+\gamma x)+$$
$$+a(l)\int_0^\infty d\xi G(\xi)\Delta I(x-\xi,y+\gamma(x-\xi))+$$
$$+b(l)\int_0^\infty d\xi\overline{G}(\xi)\int_0^\infty d\xi' G(\xi')\Delta I(x-\xi-\xi',$$
$$y+\gamma(x-\xi-\xi'))+$$
$$+c(l)\int_0^\infty d\xi\overline{G}(\xi)\Delta I(x-\xi,y+\gamma(x-\xi)), \qquad (12)$$

where

$$a(l) = \frac{[1-A(l)-C(l)][1-B(l)]}{[1-A(l)-B(l)-C(l)][1-A(l)]},$$

$$b(l) = \frac{B(l)[1-B(l)]}{[1-A(l)-B(l)-C(l)][1-A(l)]}$$

and

$$c(l) = \frac{B(l)[1-B(l)]}{[1-A(l)-B(l)-C(l)]}, \qquad (13)$$

with

$$A(l) = 1-\left(\frac{\sqrt{2}}{u}l+1\right)\exp\left\{-\frac{\sqrt{2}l}{u}\right\},$$

$$B(l) = 1-\left(\frac{l^2}{u^2}+\frac{\sqrt{2}}{u}l+1\right)\exp\left\{-\frac{\sqrt{2}l}{u}\right\}$$

and

$$C(l) = 1+\left(\frac{l^2}{u^2}+\frac{\sqrt{2}}{u}l-1\right)\exp\left\{-\frac{\sqrt{2}l}{u}\right\}. \qquad (14)$$

In the above, l represents a small integration interval, chosen on the order of u, while the function $\overline{G}(\xi)$ is given by (Fig. 1)

$$\overline{G}(\xi) = \frac{2}{u}\exp\left\{-\frac{\xi}{u}\right\}\cos\left(\frac{\xi}{u}\right). \qquad (15)$$

Identifying p as $\partial Z/\partial x$, and ΔI, through (3), as

$$\Delta I = u\frac{\partial I_2}{\partial x}+\frac{u^2}{2}\frac{\partial^2 I_2}{\partial x^2}, \qquad (16)$$

and then going back to the (X,Y) variables, we easily get from (12)

$$\mathcal{O}\{k_1(Y-\gamma X)Z(X,Y)\} =$$
$$= \mathcal{O}\left\{I(X,Y)+a(l)\int_0^\infty d\xi G(\xi)I_\xi(X,Y)\right\}+$$
$$+\mathcal{O}\left\{b(l)\int_0^\infty d\xi\overline{G}(\xi)\int_0^\infty d\xi' G(\xi')I_{\xi+\xi'}(X,Y)\right\}+$$
$$+\mathcal{O}\left\{c(l)\int_0^\infty d\xi\overline{G}(\xi)I_\xi(X,Y)\right\}, \qquad (17)$$

with

$$I(X,Y) = uI_2(X,Y)+\frac{u^2}{2}\mathcal{O}[I_2(X,Y)],$$

$$I_\xi(X,Y) = I(X-\xi,Y-\gamma\xi), \text{ and}$$
$$I_{\xi+\xi'}(X,Y) = I(X-(\xi+\xi'),Y-\gamma(\xi+\xi')), \qquad (18)$$

where the operator $\mathcal{O}$ is given by

$$\mathcal{O} = \frac{\partial}{\partial X}+\gamma\frac{\partial}{\partial Y}. \qquad (19)$$

To first order in u, equation (17) reduces finally to

$$\frac{k_1(Y-\gamma X)}{u}Z(X,Y) = I_2(X,Y)+$$
$$+a(l)\int_0^\infty d\xi G(\xi)I_2(X-\xi,Y-\gamma\xi)+$$
$$+b(l)\int_0^\infty d\xi\overline{G}(\xi)\int_0^\infty d\xi' G(\xi')I_2(X-(\xi+\xi'),$$
$$Y-\gamma(\xi+\xi'))+$$
$$+c(l)\int_0^\infty d\xi\overline{G}(\xi)I_2(X-\xi,Y-\gamma\xi)+F(\gamma X-Y), \qquad (20)$$

where $F(\cdot)$ is a generic single-argument function that cannot be recovered through our approach.

Except for the overall multiplicative factor, $k_1(Y-\gamma X)$, the above yields an estimate of the imaged surface which depends on the reflectance map parameters only via $\gamma \equiv k_2(Y-\gamma X)/k_1(Y-\gamma X)$. Since

k_1 and k_2 are functions of the arbitrary orientations $(P_0(Y-\gamma X), Q_0(Y-\gamma X))$ about which the linear expansion of the reflectance map (7) is assumed, we can use (20), with arbitrary γ values, to estimate the function $Z'(X,Y) \equiv k_1(Y-\gamma X)Z(X,Y)$, without having to know the k_i's. Once such function has been obtained, an estimation procedure similar to the one described in [5] can be employed to yield $k_1(Y-\gamma X)$, thus allowing the complete recovery of the surface function, $Z(X,Y)$, as shown next.

$Z(X,Y)$ can be formally written as

$$Z(X,Y) = \frac{u\bar{I}_2(X,Y)}{k_1}, \qquad (21)$$

where $\bar{I}_2(X,Y)$ stands for the right-hand side of (20), and where it should be kept in mind that k_1 is a function of $Y-\gamma X$.

From such expression, according to [5], we can interpret $\bar{I}_2$ as the image which would result if the irradiance pattern originating I_1 underwent a rotation by $\Theta = k_1(\gamma, 1, 0)/\bar{I}_2$, over the imaged surface, $Z(X,Y)$. Calling $R = (X,Y,Z)$ the vector position of a point in $Z(X,Y)$ (given with respect to a coordinate system with $-Z$ direction along the optical axis), and assuming orthographic imaging projection, the displacement of the surface irradiance pattern would in this case be

$$\Delta R \equiv \Theta \times R = (u, v, \Delta Z), \qquad (22)$$

since $I_1(X,Y)$ is taken into $\bar{I}_2(X+u, Y+v)$, and an unobservable displacement also results along the optical axis direction. For the above Θ, it is easy to see that (21) is recovered from (22), which also yields $\Delta Z = -k_1.(X+\gamma Y)/\bar{I}_2$.

Now, for small u and v, it is reasonable to assume that the displacement ΔR will be perpendicular to the surface normal, $\mathbf{n} = (-P, -Q, 1)/\sqrt{P^2+Q^2+1}$, at each point, which yields $\Delta R \cdot \mathbf{n} = 0$, and thus the relation

$$u\bar{I}_2(P+\gamma Q) + k_1(X+\gamma Y) = 0, \qquad (23)$$

that we can use as a constraint over k_1, by introducing the functional

$$\mathcal{F} = \int [u\bar{I}_2(P+\gamma Q) + k_1(X+\gamma Y)]^2 ds, \qquad (24)$$

to be minimized through the standard least-squares approach.

In (24), s denotes a direction perpendicular to the lines $Y-\gamma X = \beta$, for β a constant, such that k_1 does not vary along s, and can thus be taken out of the integral. It is also easy to see that we can identify $P+\gamma Q = (P'+\gamma Q')/k_1$ in that equation, where $P' = \partial Z'/\partial X$ and $Q' = \partial Z'/\partial Y$. Thus, if we rewrite $\mathcal{F}$ in terms of (P', Q'), and minimize it with respect to k_1, we finally find

$$k_1^4(Y-\gamma X) = \frac{\int [u\bar{I}_2(P'+\gamma Q')]^2 ds}{\int (X+\gamma Y)^2 ds}, \qquad (25)$$

which completes the estimation of the surface function as $Z(X,Y) = Z'(X,Y)/k_1(Y-\gamma X)$.

3 Introducing the Brightness Gradient

Here we show how the brightness gradient information can be introduced into the GSFS framework, to improve the reconstruction process. First, we note that the foregoing development, from equation (1) through (6), remains unchanged if, instead of the irradiance function, we work with any combination of its derivatives. Let us consider the particular input

$$I_1'(X,Y) = \frac{\partial I_1}{\partial X} + \gamma \frac{\partial I_1}{\partial Y} \equiv \nabla I_1 \cdot (1, \gamma), \qquad (26)$$

which corresponds to the directional derivative of the brightness function, along the direction $(1,\gamma)$. If we assume a quadratic approximation to the reflectance map, of the form

$$I_1(X,Y) = k_0 + k_1 P + k_2 Q + k_3 (P+\gamma Q)^2, \qquad (27)$$

where, as in (7), the coefficients k_i can be functions of $(Y-\gamma X)$, it is easy to see that, in terms of the variables x and y in (2), the derivative I_1' would admit the expansion

$$I_1'(x, y+\gamma x) \equiv \frac{\partial I_1}{\partial x} = k_1(y) p_x + 2k_3(y) p_x p, \qquad (28)$$

where p_x denotes the partial derivative of p with respect to x.

Now, if we assume that p_x varies slowly with x, such that $k_1(y)p_x$ and $k_3(y)p_x$ can be approximated as functions only of y, we obtain, by repeating the steps which led from equation (9) to equation (11),

$$k_1'(y)p = \Delta I' +$$

$$+ k_1'(y) \int_0^\infty G(\xi) p(x-\xi, y+\gamma(x-\xi)) d\xi, \qquad (29)$$

where $k_1'(y)$ stands for $2k_3(y)p_x$, and $\Delta I' \equiv I_1' - I_2'$, with I_2' given by

$$I_2'(x, y+\gamma x) = \int_0^\infty G(\xi) I_1'(x-\xi, y+\gamma(x-\xi)) d\xi \ . \qquad (30)$$

Now, following the reasoning that led from equation (11) to equation (21), it is easy to find the second estimate for $Z(X,Y)$, under the form

$$Z(X,Y) = \frac{u\overline{I}'_2}{k'_1} \tag{31}$$

where $\overline{I}'_2$ is given by the right-hand side of equation (20), with I_2 replaced by I'_2. The single free parameter, k'_1, in equation (31), can be estimated through the same least-squares procedure outlined at the end of Section 2. It would thus be given by expression (25), again with $\overline{I}'_2$ substituted for $\overline{I}_2$.

4 Experiments

The reconstructions that we present next have been obtained by combining the estimates (21) and (31) through the simple average

$$Z_{est}(X,Y) = \frac{u}{2}\left(\frac{\overline{I}_2}{k_1} + \frac{\overline{I}'_2}{k'_1}\right), \tag{32}$$

although we could have used a different u value with each estimate. For comparison, we will also be showing the reconstructions yielded by the standard GSFS alone (equation (21)), without the gradient information.

As test inputs, we considered images already used as benchmarks in previous works, such as those in [1] and in [6] (found at the ftp server eustis.cs.ucf.edu, under the pub/tech_paper/survey directory). Our results can thus be easily confronted with the ones yielded by other approaches (in this regard, it should always be kept in mind that, alone among all others, our algorithm does not require any reflectance map information).

The experiments presented here are for the synthetic image Mozart101, and for the real images Mannequin, Lenna1 and Lenna2 (Fig. 2). All reconstructions have been performed with $\gamma = 0$, $u = 0.05$, and $l = 0.1$. No previous segmentation of the input images was assumed.

The surface functions obtained from Mozart101 - which is a lambertian rendition of a range map, under $(1,0,1)$ illumination - are shown in Fig. 3. It is apparent there that the incorporation of the derivative information allowed a more faithful estimation of the surface shape, compensating for the irradiance non-uniformity due to the slanted illumination.

A similar remark can be made regarding the Mannequin experiment (Fig. 4). Again, the non-uniform irradiance (shadow areas) led to distortions in the standard GSFS estimate. The resulting flat nose and twisted mouth have been fairly corrected in the much more well-balanced reconstruction through the new algorithm.

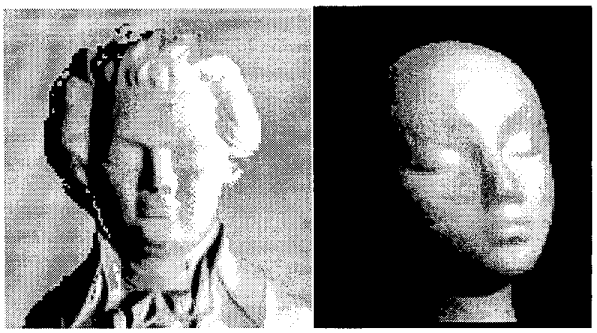

(a) (b)

(c) (d)

Fig. 2: Input images. (a) Mozart101, (b) Mannequin, (c) Lenna1, (d) Lenna2

Finally, in the two Lenna experiments (Figs. 5 and 6), the combined irradiance-gradient approach allowed a better representation of the finer features of the model, all but lost in the standard GSFS reconstruction of Fig. 6.

5 Concluding Remarks

In a previous work [2], we have proposed a new approach to shape from shading (the GSFS), recasting the process as the matching of a pair of monocular shading images, the matching image to be found from an intensity conservation relation. The shape estimate thus obtained - given as a closed-form expression for the depth function (21) - depends on the convolutions of the input image with two 1D filters, G and $\overline{G}$ (Fig. 1), which display the familiar structure of a positive-valued crest sided by a negative depression, characteristic of filters used to model the receptive fields of channels in the visual pathway (the sum $G + \overline{G}$ resembles a one-sided DOG - difference of Gaussians -

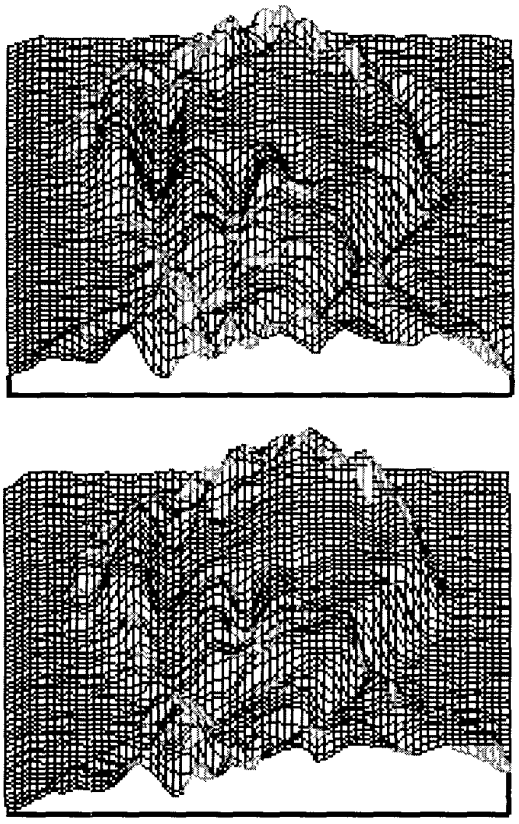

Fig. 3: Shape estimation from Mozart101. Top: Shading and Gradient Approach, Bottom: Standard GSFS

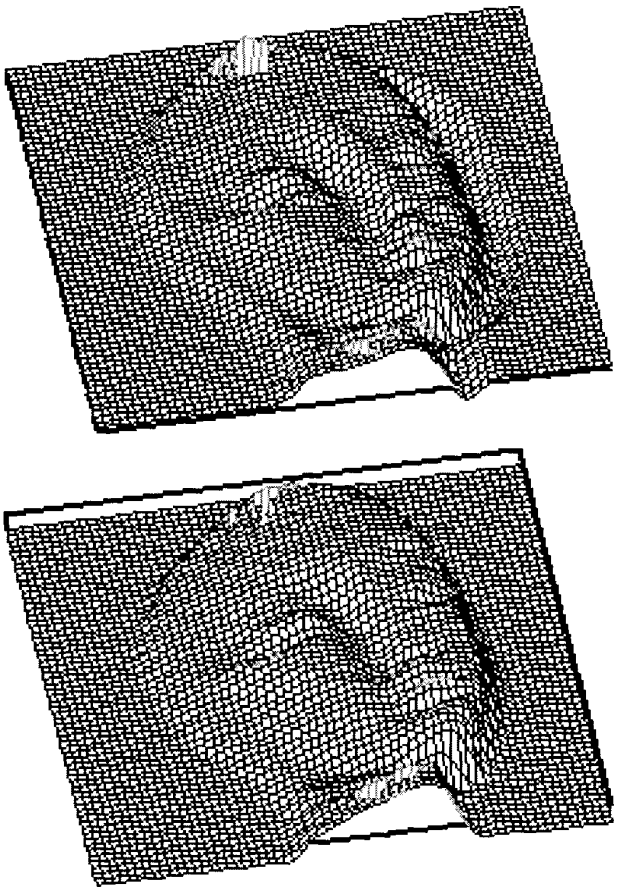

Fig. 4: Shape estimation from Mannequin. Top: Shading and Gradient Approach, Bottom: Standard GSFS

function). Moreover, for small values of their arguments (less than the matching constant, u), such filters approximate the shape of the disparity selectivity profiles of the tuned-inhibitory and the tuned-zero neurons found in the monkey's visual cortex [8], a role for which we already envisioned in the explanation of the binocular fusion of monocular images [3].

Here, we have shown how to improve GSFS, by taking into account brightness gradient information, in order to better represent the higher frequency components of the scene. This has allowed reconstructions which are more faithful to the finer details of the imaged surface, and which are somewhat shielded from non-uniform irradiance effects, such as those arising from self-shadows or slanted illumination. As a drawback, the gradient-based estimation becomes more vulnerable to image noise.

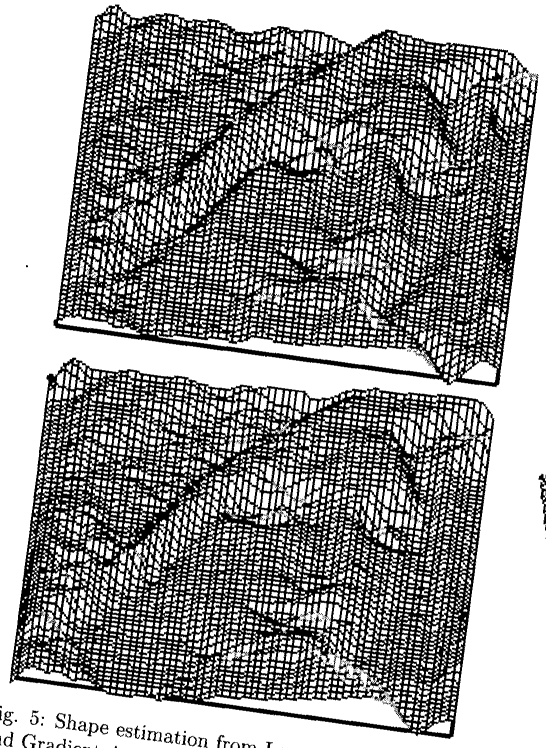

Fig. 5: Shape estimation from Lenna1. Top: Shading and Gradient Approach, Bottom: Standard GSFS

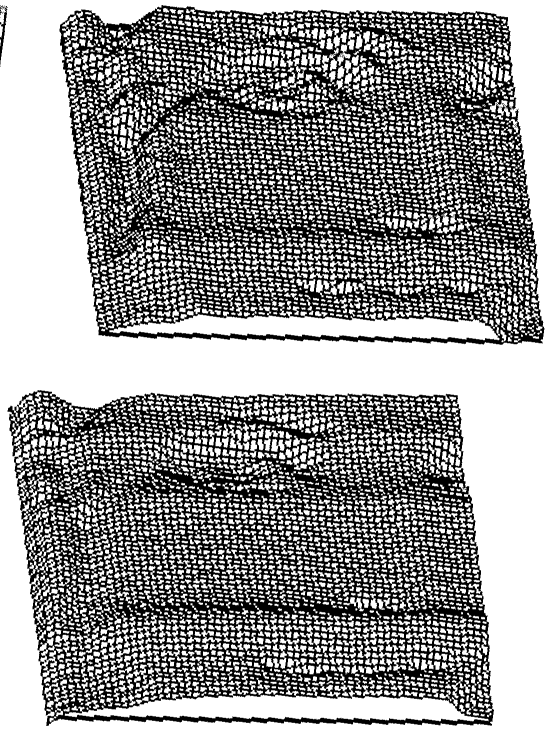

Fig. 6: Shape estimation from Lenna2. Top: Shading and Gradient Approach, Bottom: Standard GSFS

References

[1] R. Zhang, P.-S. Tsai, J.E. Cryer, and M. Shah Shape from shading: a survey, IEEE Trans. Pattern Anal. Machine Intell., 21(8) (1999) 690-706.

[2] J.R.A. Torreão A Green's function approach to shape from shading Technical Report RT-09/99, PG em Comput. Aplicada e Automação, UFF (http://www.caa.uff.br/reltec.html). Submitted for publication

[3] J.R.A. Torreão and J.L. Fernandes, Matching photometric stereo images, J. of the Optical Soc. of America A 15 (12) (1998) 2966-2975.

[4] S.T. Barnard, "A stochastic approach to stereo vision", Proc. Fifth National Conference on Artificial Intelligence, USA, 1986, pp. 676–680.

[5] J.R.A. Torreão, A new approach to photometric stereo, Patt. Recogn. Letters 20 (5) (1999) 535-540.

[6] R. Zhang and M. Shah Shape from intensity gradient, IEEE Trans. Systs. Man Cybernetics, A29(3) (1999) 318-325.

[7] A.L. Fetter and J.D. Walecka, Theoretical Mechanics of Particles and Continua, McGraw-Hill, New York, 1980

[8] G. F. Poggio, Stereoscopic processing in monkey visual cortex: a review, *in* T.V. Papathomas, C. Chubb, A. Gorea, and E. Kowler, eds. Early Vision and Beyond, The MIT Press, Cambridge, MA, 1995

Acknowledgment: Partially supported by Finep (Project Recope 0626/96-SAGE)